Tailoring the Chemical Structure of Cellulose Nanocrystals by Amine Functionalization

Rosarita D'Orsi,[a] Viviana Claudia Canale,[b] Rocco Cancelliere,[b] Omar Hassan Omar,[c] Claudia Mazzuca,[b] Laura Micheli,[b] and Alessandra Operamolla*[a, d]

The surface functionalization of cellulose nanocrystals is presently considered a useful and straightforward tool for accessing very reliable biocompatible and biodegradable nanostructures with tailored physical and chemical properties. However, to date the fine characterization of the chemical appendages introduced onto cellulose nanocrystals remains a challenge, due to the low sensitivity displayed by the most common techniques towards surface functionalization. In this paper, we demonstrate the easy functionalization of cellulose nanocrystals with aliphatic and aromatic amines, demonstrating the tunability of their properties in dependence on the selected functionality. Then, we apply to colloidal suspensions of modified nanocrystals ^{1}H NMR analysis to elucidate their surface structure. To the best of our knowledge, this is the first report where such investigation was performed on cellulose nanocrystals presenting both surface and reducing end modification. These results involve interesting implications for the fields of cultural heritage and of materials chemistry.

Introduction

Cellulose nanocrystals (CNCs) are crystalline nanostructures isolated by applying a top-down approach to native cellulose synthesized by plants or bacteria.[1] These intriguing organic nanoaggregates feature a high aspect ratio, with a diameter in the range between 5 and 50 nm and a length ranging from 100 to 500 nm. Discovered in the 1950s,[2,3] CNCs can be isolated by acid hydrolysis using sulfuric, phosphoric or halogenidric acids.[1] The interest towards these nanostructures is high, considering the plethora of applications that can be envisioned for these sustainable nanoparticles.[4–11]

Only recently, CNCs application in Cultural Heritage preservation and conservation was proposed and investigated.[12–19] In particular, cellulose nanocrystals have revealed great potential as protection and reinforcing agents for historical paper[12–14] and canvases.[15–17] This reinforcing treatment is not only compatible with the environment of conservation ateliers, since it entails only the use of sustainable and nontoxic material, but implies the easy removal of the nanocellulose coating layer by application of a cleaning hydrogel on the paper surface.[12] This possibility virtually protects paper artworks from their unavoidable erosion determined by the continuous monitoring and, especially, by the consolidation actions necessary to safeguard this legacy.

Along with the demonstration of reversibility, our previous work[12] shed an important light on the role of surface functionalization of CNCs on the conservation action, that was previously overlooked: surface sulfation,[20] introduced by the sulfuric acid hydrolysis, the most widely used protocol to access CNCs by chemical approach, yields nanocrystals that "age badly". Sulfate groups in these nanocrystals are randomly present on the primary hydroxyl groups on the surface glucopyranose units.[21] Accelerated aging experiments performed on sacrificial Whatman samples treated with sulfated CNCs (S_CNCs) and their non-sulfated (i.e. neutral) counterpart (N_CNCs) demonstrated a dangerous decrease of pH in the former samples toward an acid value (from 5.7 to 4.5), whilst the samples treated with N_CNCs displayed stable pH. We attributed this occurrence to an elimination of the sulfate group as hydrogen sulfate, catalyzed by the acid traces that, in historical samples, can derive from inks, pollutants, and organic acids arising from cellulose degradation. In this light, it appears clear that pursuing the use of S_CNCs in Cultural Heritage preservation may be hazardous. On the other side, N_CNCs can be synthesized by cellulose hydrolysis with hydrochloric acid.[22] These nanocrystals are similar in morphology to S_CNCs but lack the surface sulfation that determines pH decrease. However, N_CNCs present much lower dispersibility properties than sulfated nanocrystals: whilst S_CNCs show surface charge repulsion between negative charges formed at pH > 1.0,[23] this

[a] Dr. R. D'Orsi, Prof. A. Operamolla
Dipartimento di Chimica e Chimica Industriale
Università di Pisa
via Giuseppe Moruzzi, 13, 56124 Pisa (Italy)
E-mail: alessandra.operamolla@unipi.it

[b] V. C. Canale, Dr. R. Cancelliere, Prof. C. Mazzuca, Prof. L. Micheli
Dipartimento di Scienze e Tecnologie Chimiche
Università degli Studi di Roma Tor Vergata
Via della Ricerca Scientifica, 00133 Rome (Italy)

[c] Dr. O. Hassan Omar
CNR-ICCOM – Istituto di Chimica dei Composti Organometallici
Via Edoardo Orabona 4, 70126 Bari (Italy)

[d] Prof. A. Operamolla
Consorzio Interuniversitario Nazionale di ricerca in Metodologie e Processi Innovativi di Sintesi C.I.N.M.P.I.S.
56124 Pisa (Italy)

EurJOC
European Journal of Organic Chemistry

Research Article
doi.org/10.1002/ejoc.202201457

Chemistry Europe
European Chemical Societies Publishing

property is not displayed by N_CNCs, that aggregate quickly in water suspension. Consequently, the manipulation and characterization of N_CNCs is experimentally more difficult. Given the higher stability displayed by N_CNCs, we think it is highly desirable investigating their preparation and surface chemical functionalization. For this reason, in this work we first focus on the functionalization of N_CNCs, proposing the decoration of nanocrystals structure with aliphatic or aromatic amines. The new chemical functionalities are introduced both on the surface of the nanocrystals, applying a synthetic sequence interesting the transformation of the C_6 carbon of the glucopyranose ring, and on the reducing termini of cellulose nanocrystals, by the reductive amination reaction applied in the presence of sodium cyanoborohydride.[24] Indeed, we consider surface amination a good approach to access cellulose nanocrystals with deacidifying properties as these would mimic the action of ethanolamines (used in the Book Preservation Associates, BPA, conservation process).[25] At the same time, the decoration of N_CNCs with aromatic amines can give access to nanocrystals with photophysical properties or with potential applications in electrochemistry. However, a deep chemical surface characterization of modified N_CNCs may be tricky, for their low dispersibility and for the very low number of chemical functionalities introduced by surface chemistry. This frequently limits the true possibilities of a fine molecular characterization since there is often only access to indirect evidences of the presence of the new chemical functionality.[24] In this paper, using dimethylsulfoxide as the dispersion medium, we obtain stable colloidal suspensions of N_CNCs and of their functionalized derivatives. Then, we elucidate their surface structure applying ^{1}H NMR experiments. To the best of our knowledge, this is the first report where such investigation was performed on cellulose nanocrystals presenting reducing end modification.

Results and Discussion

We have amply demonstrated that **N_CNCs 1** can be prepared from cotton linters by aqueous HCl hydrolysis. This procedure allows to isolate nanocrystals mainly consisting of cellulose I_β crystalline phase with an average length of ~150 nm.[12,24] These

Alessandra Operamolla received her Ph.D. in Chemistry of Innovative Materials in 2009 from the University of Bari. In 2010 she received an exchange grant from the European Science Foundation for a post-doc stay at the Linz Institute for Organic Solar Cells (LIOS), Austria. In 2016, she was appointed Assistant Professor of Organic Chemistry at the University of Bari, where she started independent research on cellulose nanomaterials. In 2019, she was appointed Associate Professor of Organic Chemistry at the University of Pisa. Alessandra leads the NanoLeaves group and is interested in the application of nature-derived biopolymers as innovative materials.

nanocrystals were used as substrates for the following functionalization steps. **N_CNCs** surface modification with aliphatic amine functionalities was achieved by applying the synthetic sequence summarized in the Scheme 1.

To transform the surface primary alcoholic groups of cellulose into aliphatic secondary amines, we first converted them quantitatively into carboxylate groups. This reaction was mildly performed in water applying an oxidation process catalyzed by 2,2,6,6-tetramethylpiperidine-1-oxyl radical (TEMPO), using sodium hypochlorite as oxidant and sodium bromide as mediator.[26] At the end of the reaction, TEMPO-oxidized cellulose nanocrystals (**TO-CNCs**, **2**) were isolated in an 89% yield. Then, **TO-CNCs** were subjected to a condensation reaction with hexane-1-amine to yield the amidated nanocrystals **3** in 85% yield. For the activation of the carboxyl moieties of **TO-CNCs**, 1-ethyl-3-(3-dimethylaminopropyl) carbodiimide (EDC) was used as condensing agent and 4-(N,N-dimethylamino)pyridine (DMAP) as a base, whilst N,N-dimethylformamide was used as solvent. The last step of the sequence was a reduction of the amide functionalities to secondary amines, performed dispersing the cellulose nanocrystals **3** in anhydrous diethyl ether and using lithium aluminum hydride as reducing agent at room temperature. Through this last reaction step, performed in an inert atmosphere, we isolated surface-aminated CNCs **4** in 93% yield. This synthetic sequence, having as intermediates carboxylated CNCs, was chosen for two main reasons: the first one is that TEMPO oxidation is usually considered sustainable, since it occurs at room temperature in water with mild oxidants; the second is connected to the high yields of the TEMPO oxidation reaction, leading to highly pure products of easy isolation. The conditions for the following condensation and reduction reactions were also relevantly efficient. When dealing with CNCs, reaction yields are important, to provide isolation of products with acceptable purity and properties. Concerning the toxicity of solvents such as DMF, diethyl ether and the hazardousness of LiAlH$_4$, used here as reducing agent, certainly in the future these chemicals will be replaced by more benign alternatives, but this will require an extensive re-design of the synthetic procedure. The high efficiency of the synthetic sequence of Scheme 1 was accompanied by the easy recognizability of the chemical changes on the nanocrystals surface, followed by attenuated total reflectance Fourier transform infrared spectra (ATR-FTIR) acquired on each intermediate and on the final product, thanks to the distinguishable features of the carboxyl and amide signals, whose appearance and disappearance were taken as an indication of reaction success.

These spectra are presented in Figure 1, which displays the infrared spectra of **N_CNCs**, **TO-CNCs**, amidated nanocrystals **3**, and aminated CNCs **4** in the region 4000–500 cm^{-1}.

All spectra show the typical features of cellulose:[27,28] the large band at about 3300 cm^{-1} is attributable to OH stretching, while bands localized at 1428 cm^{-1}, 1370 cm^{-1} and 1280 cm^{-1}, are due to CH$_2$ bending, OH bending, and ring asymmetric stretching, respectively. In addition, the bands appearing at 1160 and 1053 cm^{-1} arise from C−O−C asymmetric stretching of the glucopyranose ring. Lastly, the 896 cm^{-1} band is attribut-
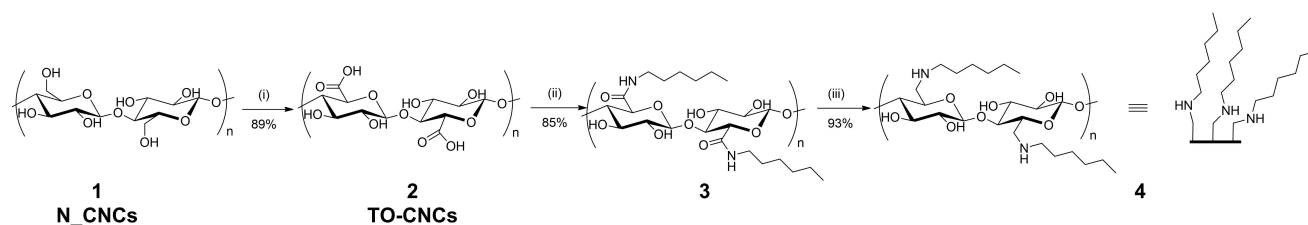
Scheme 1. Synthesis of **4** from **N_CNCs**. Reaction conditions: (i) NaClO aq 15%, NaBr, TEMPO radical, NaOH, pH 11, r.t.; (ii) hexaneamine, 1-ethyl-3- (3-dimethylaminopropyl)carbodiimide (EDC), 4-(N,N-dimethylamino)pyridine (DMAP), DMF, r.t.; (iii) lithium aluminium hydride 1.0 M in Et$_2$O, dry Et$_2$O, 0 °C to r.t.
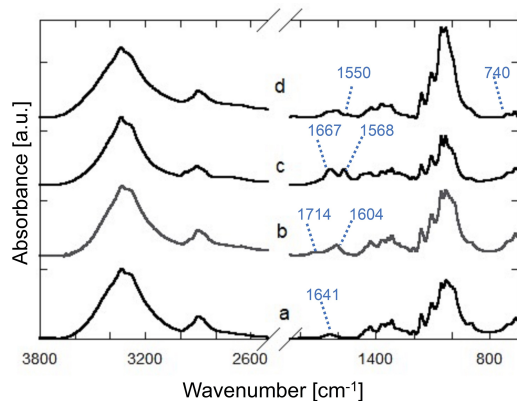

Figure 1. FTIR spectra of a) **N_CNCs**, b) **TO-CNCs**, c) **3**, and d) **4**.

able to the deformation mode of anomeric CH in cellulose. The absorption band observed at 1641 cm^{-1} is due to the bending of absorbed water, usually found in each nanocellulose sample. The functionalization of **N_CNCs** can be easily detected by FTIR spectra (Figures 1 and S1). Indeed, the spectrum of **TO-CNCs** shows the characteristic absorption bands of carboxylic groups (in the acidic and deprotonated forms) at about 1714 cm^{-1} (acidic form) and 1604 cm^{-1} (salt form).[29] Amide groups in nanocrystals **3** are easily detectable thanks to the appearance in the spectrum of the Amide I band at about 1667 cm^{-1}, and of the Amide II band at 1568 cm^{-1}.[30,31] Finally, the spectrum of nanocrystals **4** shows bands at about 1550 cm^{-1} and 740 cm^{-1}, attributable to bending and wagging of NH groups

respectively[28,32] Furthermore, from FTIR spectra, it is possible to estimate the crystallinity of samples through the ratio of the intensities of bands centered at 1427 cm^{-1} and 898 cm^{-1}.[33] Crystallinity does not change following the functionalization in an appreciable manner, as these ratios for **N_CNCs 1**, **TO_CNC 2**, amidated CNCs **3** and aminated CNCs **4** are 1.20 ± 0.10, 1.25 ± 0.15, 1.30 ± 0.10, and 1.20 ± 0.15 respectively.

Then, we decided to evaluate the reductive amination reaction on N_CNCs and its potentialities both in developing cellulose nanocrystals with tunable basicity properties or decorated with terminal aromatic moieties. We selected two aliphatic amines, hexane-1-amine **5a** and octane-1,8-diamine **5b**, and two primary amines with pending aromatic structures, dopamine (2-(3,4-dihydroxyphenyl)ethanamine) **5c** and pyrene-1-amine **5d**. The corresponding synthesis of products **6a–d** is depicted in Scheme 2. The reductive amination reaction is the ideal protocol to allow modification only of CNCs' reducing ends, leaving the remaining nanocrystal surface unfunctionalized and eventually available for further chemical manipulation. As displayed in Scheme 2, the reductive amination reaction, carried out at pH 6.0 in the presence of sodium cyanoborohydride as the reducing agent, yielded products **6a–d** in high yields. This reduction protocol allowed to avoid the use of hydrogen and supported metallic catalysts, that would introduce difficulties in cellulose purification.

Whilst in the case of the synthetic sequence of Scheme 1, ATR-FTIR was a satisfying technique for assessing the success of each reaction step, in the case of reductive amination and of the corresponding products, this analysis was not as awardable as in the previous case. This was basically due to the low
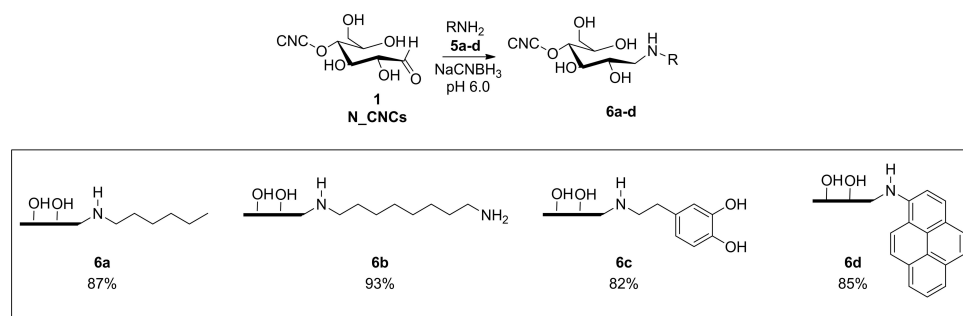
Scheme 2. Synthesis of reductively aminated **N_CNCs 6a–d**. Reaction conditions: **N_CNCs**, primary amine (RNH$_2$ is: hexane-1-amine **5a**, octanediamine-1,8 **5b**, dopamine **5c**, or pyrene-1-amine **5d**), sodium cyanoborohydride, aqueous phosphate buffer 50 mM, pH 6.0, r.t.

sensitivity of the technique towards the new low abundant functionalities introduced during the reactions. Topochemical reactions on nanocellulose, such as the ones performed in this study, imply reactivity at the solid-liquid interface. This often introduces a very low degree of substitution (DS) and difficulties to find characterization techniques with enough sensitivity to reveal the new functionalities. Considering these experimental limits, we decided to attempt the acquisition of ^{1}H NMR spectra of our cellulose nanocrystals in colloidal dispersion to get information about their more mobile surface structures. So far, such spectra were acquired by Jiang et al. in deuterated water,[34] but our samples rapidly precipitated from water. Therefore, we decided to use d_6-DMSO, a solvent able to yield more stable suspensions, to enable these studies at 65 °C. The spectrum of **N_CNCs 1** is reported in Figure 2. The signals recorded for this sample are in line with the signals found by other authors for nanocellulose[34] and cellulose:[35] the anomeric proton (H1) produces a signal between 4.37–4.21 ppm, the methylene C_6-OH unit two signals of diastereotopic protons (H6) at 3.91–3.71 ppm. The cluster of H3, H4, H5 signals appears between 3.71–3.47 ppm and the H2 signal is centered at 3.35 ppm. No signal from hydroxyl groups is detectable, due to rapid exchange with the solvent: in our experiment, water was originated by the nanocrystals themselves, which incorporate crystallized water upon drying. This water is also visible in the FTIR spectra (Figure 1, absorption band centered at 1641 cm^{-1}). Cellulose nanocrystals after surface amination **4** present a quite different ^{1}H NMR spectrum, still conserving a signal in the region of the anomeric proton but showing the disappearance of the two signals attributed to the diastereotopic methylene C_6-OH. This is reasonable, since at the end of the reaction sequence C_6 will not anymore be linked to a hydroxyl group but rather to a secondary amine group. Consequently, a shift to a more shielded field of the diastereotopic protons signals may arise. At the same time, the spectrum of sample **4** showed the characteristic appearance of a cluster of aliphatic signals between 3.3 and 1.0 ppm, attributed to the hexyl chains.

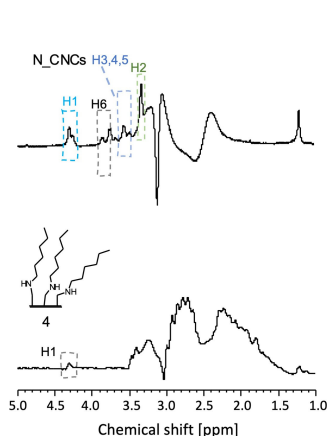Once optimized the acquisition conditions for samples **1** and **4**, we applied the same analysis to samples **6a–d**. The relevant spectra, except for nanocrystals **6b** that yielded a featureless spectrum (compare Figure S5), are reported in the Figure 3.

The almost featureless spectrum of **6b** was justified based on this sample's scarce solubility: we hypothesize that the use of an aliphatic diamine as reaction partner had promoted in sample **6b** an unwanted cross-linking reaction between termini of different nanocrystals. This basically impedes any colloidal dispersion spectral analysis. The sample **6a**, terminally coupled to hexane-1-amine, shows conserved signals from the cellulosic protons, though they are detected with lower intensity: δ_H 3.34 (H2), 3.59 (H3, H4, H5), 3.78 (H6) and 4.32 (anomeric proton) ppm. These signals are also conserved in the spectra of **6c,d**. Furthermore, new signals appear in **6a** at δ_H 4.44, 4.55, 5.13 and 6.21 ppm. In the case of proton spectra of products **6c,d**, the number of new signals increased, also in intensity, appearing as a distinctive group of signals centered at δ_H 4.44, 4.54, 4.69, 4.83, 5.12, 6.10 ppm. The origin of the complex appearance of the protonic spectra in the region between 4.4 and 6.0 ppm is doubtful. Similar signals were reported by Tang et al.,[36] without furnishing any explanation about their origin. However, these signals probably correspond to alcoholic protons of D-glucopyranose and aminic protons recorded in DMSO.[37] We can hypothesize that the reaction has originated some surface structural changes that have affected the rate of exchange of the surface protons with the solvent. These signals are not present in the native nanocrystals and may have been generated by interaction of **N_CNCs** with the specific reaction medium of reductive amination. More in-deep and systematic investigation will be necessary in the future to understand the influence of the reaction on the exchange rate of these protons. Reassuringly, the high reaction yields (Scheme 2) and the clear appearance of aromatic signals in the spectra of products **6c** and **6d**, corresponding to the aromatic protons of dopamine ring[38] and of pyrene,[39] reveal the certain anchorage of the wanted functionalities on cellulose nanocrystals. Another important observation concerns the complete disappearance of signals multiplicity concerning aromatic protons of dopamine
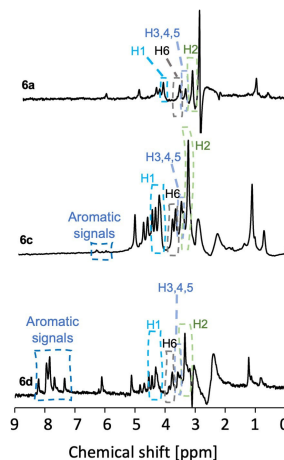

Figure 2. ^{1}H NMR spectra of **N_CNCs** and **4** (**N_CNCs** after surface amination) recorded in DMSO at 65 °C. Distortions in the spectra are due to solvent signals suppression (water, $\delta_H \sim$ 3.11 ppm and DMSO, $\delta_H \sim$ 2.46 ppm).

Figure 3. ^{1}H NMR spectra of reductively aminated **N_CNCs**, recorded in DMSO at 65 °C.

EurJOC
European Journal of Organic Chemistry

Research Article
doi.org/10.1002/ejoc.202201457

Chemistry
Europe
European Chemical
Societies Publishing

and pyrene-1-amine, once they are chemically bonded to N_ CNCs. For comparison, spectra of the two amines **5c,d**, acquired in d_6-DMSO, are reported in Figures S8 and S9. This fact is particularly evident in the spectrum of **6d**. The loss of multiplicity is accompanied by signal broadening, an occurrence which represents a further indication of the polymeric nature of the products under investigation.

The truthfulness of our conclusions made on the basis of ATR-FTIR and ^{1}H NMR analyses was supported by the FE-SEM investigation, that we carried out on each sample, to demonstrate the preserved nanocrystals morphology. The relevant micrographs are reported in Figure 4. Each sample was deposited from a $1 \, mg \, L^{-1}$ DMSO suspension of cellulose nanocrystals, for homogeneity with respect to NMR analyses. As a first observation, the diverse surface functionalization dramatically affected the aggregation tendency of CNCs. Sample **4** showed the highest tendency to form large aggregates. Although the average length of CNCs in this sample was conserved (157 ± 24 nm of **4** versus 151 ± 18 nm of **N_CNCs**), in this sample a slight increase in CNCs diameter was also visible. This result was in accordance with our previous investigation on CNCs surface esterification, and compatible with the effects of a surface functionalization with aliphatic chains.[8]

Concluding our structural investigation on the aminated products, we wanted to understand if the novel functionalized cellulose nanocrystals displayed the desired properties. First, we took into consideration cellulose nanocrystals **4**, **6a**, and **6b**. These products were designed specifically for prospective application in the conservation of historical paper. These nanocrystals are expected to display consolidating properties similar to the ones displayed by **N_CNCs**,[12] but with additional deacidifying activity. For this reason, we modulated by synthetic design the number of pending amino groups linked to the nanocrystals. In this way, we achieved the synthesis of CNCs with tailored pH, as represented in the Table 1.

These materials may be useful for the treatment of historical artworks with specific acidification problems. Whilst the N_

Table 1. pH of cellulose nanocrystals functionalized with aliphatic amines, measured in distilled water.

Sample	N_CNCs	6a	6b	4
pH	7.1 ± 0.1	6.9 ± 0.1	7.2 ± 0.3	7.3 ± 0.1

CNCs displayed pH value of 7.1, close to neutrality, the new products showed increasing pH, measured in MΩ water, depending on the number of amino functionalities introduced during the chemical synthesis. In particular, **6a** has the lowest number of secondary amine functionalities, and displayed a pH value of 6.9, close to neutrality (within the range of experimental error, imposable to **N_CNCs**). **6b** is linked to a diamine, that can either expose the second -NH$_2$ functionality to the solution or, most probably, considering the lower dispersibility of this sample, could have generated cross-linking between termini of different nanocrystals during the reaction. This sample displayed, as expected, an increase in pH to 7.2. The sample with the highest deacidifying potential was sample **4**, possessing surface amination, and thus the highest number of secondary amine groups on the surface of the nanocrystals. For this sample, the measured pH was 7.3.

The functionalization of cellulose nanocrystals with pyrene moieties may generate systems with interesting photophysical properties. Therefore here we acquired both absorption and emission spectra of **N_CNCs**, **6d** and pyrene-1-amine **5d** for preliminarily assessing their photophysical properties. The choice of DMSO as solvent not only supported the effective dispersion of cellulose nanocrystals, but also the formation of pyrene excimers, necessary to appreciate emission from this system in the visible region (~450 nm, blue emission). In our previous work,[24] we had used a pyrenyl derivative with a pending aliphatic linker, that displayed a very weak capacity to generate excimers. In this work, we use pyrene-1-amine, which displays a strong tendency to form π-stacked aggregates. The introduction of pyrene units on the cellulose nanocrystals **6d**
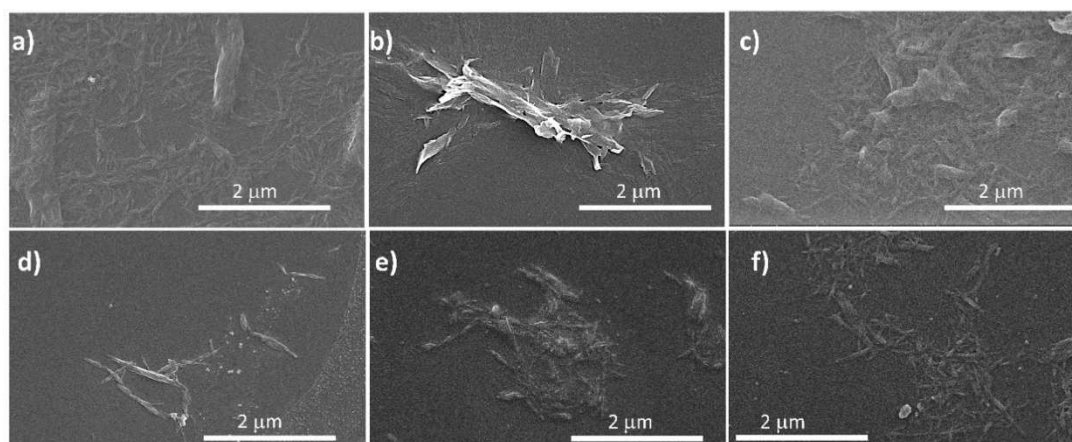

Figure 4. FE-SEM micrographs of a) **N_CNCs**, average length 151 ± 18 nm; b) **4**, **N_CNCs** modified by surface amination, average length 157 ± 24 nm; c) **6a**, **N_CNCs** terminally functionalized by hexane-1-amine, average length 157 ± 28 nm; d) **6b**, **N_CNCs** terminally functionalized by 1,8-octanediamine, average length 150 ± 23 nm; e) **6c**, **N_CNCs** terminally functionalized by dopamine, average length 135 ± 20 nm; and f) **6d**, **N_CNCs** terminally functionalized by pyrene-1-amine, average length 135 ± 12 nm. Samples were deposited on glass from DMSO suspensions at a concentration of $1 \, mg \, L^{-1}$. Scale bar: 2 µm.

EurJOC
European Journal of Organic Chemistry

Research Article
doi.org/10.1002/ejoc.202201457

Chemistry Europe
European Chemical Societies Publishing

modifies their absorption profile, causing the appearance of a wide absorption band between 250 and 450 nm (Figure 5a), not present in **N_CNCs** and clearly attributable to pyrene-1-amine **5d**. Upon excitation at 369 nm wavelength, the functionalized system displays the appearance of a distinctive emission band centered at 450 nm (Figure 5b). This emission is clearly attributed to pyrene-1-amine **5d**, covalently linked to cellulose nanocrystals termini.

In the case of product **6c**, consisting of cellulose nanocrystals terminally linked to dopamine, this system was initially synthesized in view of producing adhesives based on the polydopamine polymer[40] blended to cellulose nanocrystals as reinforcing fillers, with the intention to evaluate the effect of covalent linkage among CNCs and dopamine. However, none of our attempts to polymerize dopamine in product **6c**, followed
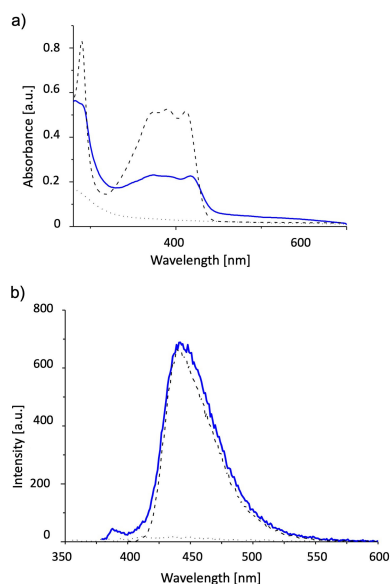

Figure 5. a) UV-Visible spectra, collected from DMSO suspensions, of **6d** (blue line 0.2 mg mL^{-1}), pyrene-1-amine **5d** (black dashed line 6.45×10^{-3} mg mL^{-1}), and **N_CNCs 1** (black dotted line 0.2 mg mL^{-1}); b) emission spectra recorded in DMSO of **6d** (blue line, 1.82×10^{-2} mg mL^{-1}), pyrene-1-amine **5d** (black dashed line, 6.45×10^{-3} mg mL^{-1}) and N_CNCs (black dotted line, 0.2 mg mL^{-1}), and. Excitation wavelength 369 nm.
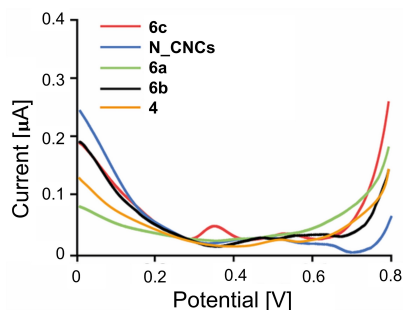

Figure 6. Electrochemical analysis using screen printed electrodes of dopamine-modified nanocellulose **6c** compared to non-modified or other aliphatic amine-modified nanocellulose. Square wave voltammetry was used as electrochemical technique in KCl 0.1 M (scan rate 1 mV s^{-1}).

by UV-Vis absorption spectroscopy, was successful. We attributed this behavior to the constraint imposed on the dopamine structure by the covalent bond established with cellulose's terminal units. Since unbound dopamine promptly polymerizes on cellulose nanocrystals,[41] this was taken as another effective demonstration of the covalent link between CNCs and the amino appendages. Therefore, this functionalized nanocellulose system can be more feasible for electrochemical applications. Square Wave Voltammetry (SWV) was the electrochemical technique used for the detection and the quantification of dopamine covalently linked to CNCs. The electrochemical measurements were performed on cellulose nanocrystals water suspensions with in-house produced screen-printed electrodes (SPEs), that included graphite working and counter electrodes as well as an Ag/AgCl reference electrode.[42] The relative current-potential curves are shown in Figure 6. Other samples, **N_CNCs**, **4**, **6a** and **6b**, were tested to ascertain that the only sample producing a signal was **6c**, the only one containing covalently linked dopamine. Indeed, the characteristic oxidation peak (0.35 V) of dopamine to its quinone, appears in the voltammogram of **6c**. An electrochemical sensor based on screen-printed electrodes was also developed to determine the unknown concentration of dopamine in modified nanocellulose. Specifically, using fixed concentrations of standard dopamine, a calibration line, reported in Figure S10, was constructed, yielding very promising analytical performances: detection limit (LOD) 0.05 µM, quantification limit (LOQ) 0.14 µM, linear Range (LR) 0.05–100 µM and high reproducibility (RSD < 7%). Using the sensor, a concentration of 0.16 µM of nanocellulose-incorporating dopamine was estimated in a suspension of **6c** 1 mg mL^{-1} (approximately 1 dopamine unit every ~3×10^4 glucopyranose units) with an accuracy of 8%. The electrochemical sensor allowed us to achieve dopamine quantification in sample **6c**, a result that was not attainable by elemental analyses, because of their insufficient sensitivity towards samples with very low nitrogen content.

Conclusion

In this work, we demonstrate that amine functionalization of cellulose nanocrystals is a useful tool to modulate their properties, to endow them with deacidifying, photophysical or electrochemical activity. Furthermore, we go into detail of the structural characterization of the functionalized cellulose nanocrystals, performing, for the first time, a successful ^{1}H NMR investigation on the reducing end functionalization of CNCs carried out on their colloidal suspensions. The dopamine presence on product **6c** is also demonstrated by square wave voltammetry. These promising results open the way to new applications of modified cellulose nanocrystals in different fields, including protection of Cultural Heritage, materials science and electrochemical sensors and devices.

EurJOC
European Journal of Organic Chemistry

Research Article
doi.org/10.1002/ejoc.202201457

Chemistry Europe
European Chemical
Societies Publishing

Experimental Section

All reagents, including amines **5a–d**, were purchased at the highest commercial quality and used without further purification. Reactions were carried out under a nitrogen atmosphere only when stated. Diethyl ether was distilled immediately prior to use on sodium and benzophenone. Anhydrous grade N,N-dimethylformamide was used and dispensed under nitrogen. Avicel PH-101 was used as the starting material for nanocrystalline cellulose isolation. Sonication of nanocellulose suspensions was carried out with a Branson Sonifier 250. Dialysis was carried out at room temperature against deionized water in nitrocellulose tubes with a cut off of 12600 Da. **S_CNCs** and **N_CNCs** were synthesized as described elsewhere.[12,24] For the evaluation of reaction yields, molar quantification was done considering the weight of anhydro glucose (AGU) unit for each sample, since the surface modification with the low degree of substitution produced is not expected to modify molecular weight of repetitive unit of cellulose in an appreciable manner.

Synthesis of 2 (TO-CNCs): In a 100 mL beaker 1.022 g of N_CNCs (6.2 mmol) were suspended in a 60 mL of deionized water using a tip sonicator (Duty Cycle constant, Power 80 W for 10 minutes). The suspension was transferred to a 250 mL three-necked round-bottomed flask equipped with two dropping funnel and a pHmeter and the pH of the dispersion was raised to 11 adding the required amount of a NaOH 3.0 N solution. Then, 95 mg of NaBr (0.926 mmol) and 96 mg of TEMPO radical (0.617 mmol) were added to the mixture. The system was mixed for further 10 minutes, before starting the dropwise addition of a NaClO 15% aqueous solution (25 mL, 49 mmol). During the reaction, the pH was constantly monitored and adjusted to 11 by adding NaOH 3.0 N. The reaction was stopped when further addition of aq. NaClO did not cause any pH decrease. The reaction was quenched adding HCl 1.0 N until the pH became 3. The mixture was transferred centrifuged for 10 minutes at 4000 rpm. The solid material was resuspended in deionized water (50 mL) and dialyzed against distilled water using a cellulose nitrate membrane with a molecular weight cut-off of 12 400 Da. Water was distilled under reduced pressure and a white solid was isolated (0.913 g, 89% yield).

Synthesis of 3: In a 100 mL three-necked round-bottomed flask 331 mg of **TO-CNCs** (1.9 mmol) were suspended in a 60 mL of anhydrous DMF. The mixture was homogenized using a bath sonicator for 10 minutes. Then, 7.92 g of EDC (51 mmol) and 6.23 g of DMAP (51 mmol) were added to the mixture. The system was kept under agitation at room temperature for 15 minutes and hexane-1-amine (1.9 mL, 14.1 mmol) was added dropwise. The system was kept under mixing at room temperature for 1 day. At the end of this period 20 mL of ethyl acetate were added to precipitate cellulose nanocrystals. The precipitate was collected after centrifugation at 4000 rpm for 10 minutes, and washed four times with fresh ethyl acetate applying four resuspension/centrifugation cycles. The solid material was resuspended in deionized water (30 mL) and dialyzed against distilled water using a cellulose nitrate membrane with a molecular weight cut-off of 12 400 Da. Water was distilled under reduced pressure and a white solid was isolated (282 mg, 85% yield).

Synthesis of 4: In a 100 mL three-necked round-bottomed flask, equipped with a water condenser and a dropping funnel, 111 mg of amidated CNCs (0.62 mmol) were suspended in a 15 mL of anhydrous diethyl ether. The mixture was cooled to 0 °C and 1.23 mL of a LiAlH₄ 1 M solution in Et₂O, diluted with further 5 mL of anhydrous Et₂O, were added dropwise. After 30 minutes at 0 °C, the mixture was warmed to r.t. and stirred for 1 day. After this reaction time, the mixture was centrifuged at 4000 rpm for 10 minutes. The precipitate was collected and washed three times with deionized water applying three resuspension/centrifugation

cycles. The solid material was resuspended in deionized water (15 mL) and dialyzed against distilled water using a cellulose nitrate membrane with a molecular weight cut-off of 12 400 Da. The suspension was freeze-dried and a white solid was isolated (103 mg, 93% yield).

Synthesis of 6a: In a 20 mL vial 260 mg of **N_CNCs** (1.6 mmol) were suspended in a 50 mM phosphate buffer (pH = 6, 10 mL) using a tip sonicator (Duty Cycle constant, Power 40 W for 10 minutes). The suspension was transferred to a 100 mL three neck round bottom flask and diluted with further 40 mL of phosphate buffer. The mixture was conditioned by nitrogen bubbling for 10 minutes. After, hexane-1-amine (0.107 mL, 0.8 mmol) was added under a nitrogen flux, followed by 163 mg of NaBH₃CN (2.4 mmol). The mixture was stirred at room temperature for 72 h. After this time, the mixture was dialyzed against distilled water using a cellulose nitrate membrane with a molecular weight cut-off of 12 400 Da. Water was distilled under reduced pressure and a white solid was isolated (228 mg, 87% yield).

Synthesis of 6b: In a 20 mL vial 260 mg of **N_CNCs** (1.6 mmol) were suspended in a 50 mM phosphate buffer (pH = 6, 10 mL) using a tip sonicator (Duty Cycle constant, Power 40 W for 10 minutes). The suspension was transferred to a 100 mL three-necked round-bottomed flask and diluted with further 40 mL of phosphate buffer. The mixture was conditioned by nitrogen bubbling for 10 minutes. After, hexane-1-amine (211 mg, 1.5 mmol) was added under a nitrogen flux, followed by 150 mg of NaBH₃CN (2.3 mmol). The mixture was stirred at room temperature for 72 h. After this time, the mixture was dialyzed against distilled water using a cellulose nitrate membrane with a molecular weight cut-off of 12 400 Da. Water was distilled under reduced pressure and a white solid was isolated (244 mg, 93% yield).

Synthesis of 6c: In a 20 mL vial 250 mg of **N_CNCs** (1.6 mmol) were suspended in a 50 mM phosphate buffer (pH = 6, 15 mL) using a tip sonicator (Duty Cycle constant, Power 40 W for 10 minutes). The suspension was transferred to a 100 mL three-necked round-bottomed flask and diluted with further 10 mL of phosphate buffer. The mixture was conditioned by nitrogen bubbling for 10 minutes. After, dopamine hydrochloride (25 mg, 0.13 mmol) was added under a nitrogen flux, followed by 50 mg of NaBH₃CN (0.8 mmol). The mixture was stirred at room temperature for 72 h. After this time, the mixture was dialyzed against distilled water using a cellulose nitrate membrane with a molecular weight cut-off of 12 400 Da. Water was distilled under reduced pressure and a white solid was isolated (206 mg, 82% yield).

Synthesis of 6d: In a 20 mL vial 250 mg of **N_CNCs** (1.6 mmol) were suspended in a 50 mM phosphate buffer (pH = 6, 15 mL) using a tip sonicator (Duty Cycle constant, Power 40 W for 10 minutes). The suspension was transferred to a 100 mL three-necked round-bottomed flask and diluted with further 10 mL of phosphate buffer. The mixture was conditioned by nitrogen bubbling for 10 minutes. After, 1-aminopyrene (25 mg, 0.11 mmol) was added under a nitrogen flux, followed by 50 mg of NaBH₃CN (0.8 mmol). The mixture was stirred at room temperature for 72 h. After this time, the mixture was dialyzed against distilled water using a cellulose nitrate membrane with a molecular weight cut-off of 12 400 Da. Water was distilled under reduced pressure and a white solid was isolated (210 mg, 85% yield).

ATR-FTIR Analyses: ATR-FTIR spectra were acquired on a Thermo Scientific (mod. Is50) instrument (Thermo Fischer Scientific, Madison, USA), equipped with a single reflection attenuated total reflectance (ATR) diamond cell for measurement in the 4000–525 cm⁻¹ region. A total of 64 scans were collected at a resolution

EurJOC
European Journal of Organic Chemistry

Research Article
doi.org/10.1002/ejoc.202201457

Chemistry
Europe
European Chemical
Societies Publishing

of 4 cm^{-1} for each sample. ATR-FTIR spectra were recorded in triplicate.

FE-SEM images: Field Emission Scanning Electron Microscopy investigation was performed using a FEI FEG-Quanta 450 instrument (Field Electron and Ion Company, Hillsboro, OR, USA). The cellulose nanocrystals were deposited on glass from DMSO suspension, at a concentration of 1 mg L^{-1}. The samples were sputtered with platinum before analysis. The cellulose nanocrystals length was measured using the software Image J 1.53e, Institute of Health, USA, on micrographs with 120000×magnification. Standard deviation was calculated on the average of >30 measurements.

pH detection: pH measurements were carried out on a suspension of 5 mg of samples in 400 μL of bidistilled water by using a Crison Instrument Basic 20 pH meter with a combined glass electrode Ag/AgCl and a porous PTFE diaphragm (Crison Instruments, Spain). Each measurement was performed in triplicate.

UV-Vis spectroscopy: UV-vis absorption measurements were performed in DMSO at room temperature using a JASCO V-750 spectrophotometer and 0.1 cm path quartz cuvettes on cellulose nanocrystals suspensions in DMSO 0.2 mg mL^{-1}.

Emission Spectroscopy: Fluorescence spectra were recorded on a Cary Eclipse Instrument with the software Scan. Spectroscopic grade DMSO was used as a solvent for the analysis. Excitation wavelength was 369 nm. Cellulose nanocrystals were analysed at a concentration of 1.82×10^{-2} mg/mL, in 1 cm cuvettes. Pyrene-1-amine was analysed at a concentration of 6.45×10^{-3} mg/mL.

^{1}H NMR Spectroscopy: To perform ^{1}H NMR experiments, 15 mg of samples were suspended in 0.7 mL of DMSO-d$_6$ (99.96 % D) using a tip sonicator (Duty Cycle constant, Power 60 W for 60 seconds). Proton spectra were obtained using a JEOL YH spectrometer with a probe operating at 500 MHz and 65 °C. Typical conditions of solvent suppression experiment employed were 5 s relaxation delay, 256 or more scans, wet number 2 and the offset were around 3.11 and 2.46 ppm relative to the H$_2$O and DMSO resonance respectively. The spectra were analysed using JEOL Delta software.

Square Wave Voltammetry: The electrochemical measurements were carried out using in-house-produced SPEs. Square-wave voltammetry (SWV) analysis were performed using a Palmesens4™ portable potentiostat system (Palmesens, Houten, The Netherlands) together with proprietary software PSTrace (Palmesens, Houten, The Netherlands).

Acknowledgements

Conflict of Interest

The authors declare no conflict of interest.

Data Availability Statement

The data that support the findings of this study are available in the supplementary material of this article.

Keywords: cellulose nanocrystals · nuclear magnetic resonance · organic synthesis · reductive amination

[1] Y. Habibi, L. A. Lucia, O. J. Rojas, *Chem. Rev.* **2010**, *110*, 3479–3500.
[2] B. G. Rånby, *Disc. Farad. Soc.* **1951**, *11*, 158–164.
[3] O. A. Battista, S. Coppick, J. A. Howsmon, F. F. Morehead, W. A. Sisson, *Ind. Eng. Chem.* **1956**, *48*, 333–335.
[4] L. Spagnuolo, R. D'Orsi, A. Operamolla, *ChemPlusChem* **2022**, *87*, e20220024.
[5] F. Milano, M. R. Guascito, P. Semeraro, S. Sawalha, T. Da Ros, A. Operamolla, L. Giotta, M. Prato, L. Valli, *Polymer* **2021**, *13*, 243.
[6] S. Sawalha, F. Milano, M. R. Guascito, S. Bettini, L. Giotta, A. Operamolla, T. Da Ros, M. Prato, L. Valli, *Carbon* **2020**, *167*, 906–917.
[7] A. Operamolla, *Intern. J. Photoen.* **2019**, *2019*, 16.
[8] A. Operamolla, S. Casalini, D. Console, L. Capodieci, F. Di Benedetto, G. V. Bianco, F. Babudri, *Soft Matter* **2018**, *14*, 7390–7400.
[9] A. Barhoum, P. Samyn, T. Ohlund, A. Dufresne, *Nanoscale* **2017**, *9*, 15181–15205.
[10] A. Dufresne, *Mater. Today* **2013**, *16*, 220–227.
[11] H. Golmohammadi, E. Morales-Narvaez, T. Naghdi, A. Merkoci, *Chem. Mater.* **2017**, *29*, 5426–5446.
[12] A. Operamolla, C. Mazzuca, L. Capodieci, F. Di Benedetto, L. Severini, M. Titubante, A. Martinelli, V. Castelvetro, L. Micheli, *ACS Appl. Mater. Interfaces* **2021**, *13*, 44972–44982.
[13] Q. Xu, G. Poggi, C. Resta, M. Baglioni, P. Baglioni, *J. Colloid Interface Sci.* **2020**, *576*, 147–157.
[14] L. Bergamonti, M. Potenza, A. H. Poshtiri, A. Lorenzi, A. M. Sanangelantoni, L. Lazzarini, P. P. Lottici, C. Graiff, *Carbohydr. Polym.* **2020**, *231*, 8.
[15] K. Kolman, O. Nechyporchuk, M. Persson, K. Holmberg, R. Bordes, *ACS Appl. Nanomater.* **2018**, *1*, 2036–2040.
[16] O. Nechyporchuk, K. Kolman, A. Bridarolli, M. Odlyha, L. Bozec, M. Oriola, G. Campo-Frances, M. Persson, K. Holmberg, R. Bordes, *Carbohydr. Polym.* **2018**, *194*, 161–169.
[17] A. Bridarolli, M. Odlyha, O. Nechyporchuk, K. Holmberg, C. Ruiz-Recasens, R. Bordes, L. Bozec, *ACS Appl. Mater. Interfaces* **2018**, *10*, 33652–33661.
[18] N. Gomez, S. M. Santos, J. M. Carbajo, J. C. Villar, *BioResources* **2017**, *12*, 9130–9142.
[19] S. M. Santos, J. M. Carbajo, N. Gomez, E. Quintana, M. Ladero, A. Sanchez, G. Chinga-Carrasco, J. C. Villar, *J. Mater. Sci.* **2016**, *51*, 1541–1552.
[20] N. Lin, A. Dufresne, *Nanoscale* **2014**, *6*, 5384–5393.
[21] P. Lu, Y. L. Hsieh, *Carbohydr. Polym.* **2010**, *82*, 329–336.
[22] H. Y. Yu, Z. Y. Qin, B. L. Liang, N. Liu, Z. Zhou, L. Chen, *J. Mater. Chem. A* **2013**, *1*, 3938–3944.
[23] J. F. Revol, H. Bradford, J. Giasson, R. H. Marchessault, D. G. Gray, *Int. J. Biol. Macromol.* **1992**, *14*, 170–172.
[24] O. Hassan Omar, R. Giannelli, E. Colaprico, L. Capodieci, F. Babudri, A. Operamolla, *Molecules* **2021**, *26*, 5032.
[25] H. A. Carter, *J. Chem. Educ.* **1996**, *73*, 417.
[26] H. Fukuzumi, T. Saito, T. Wata, Y. Kumamoto, A. Isogai, *Biomacromolecules* **2009**, *10*, 162–165.
[27] F. Carrillo, X. Colom, J. J. Suñol, J. Saurina, *Eur. Polym. J.* **2004**, *40*, 2229–2234.
[28] M. Rahimi, S. Shojaei, K. D. Safa, Z. Ghasemi, R. Salehi, B. Yousefi, V. Shafiei-Irannejad, *New J. Chem.* **2017**, *41*, 2160–2168.
[29] E. Lasseuguette, *Cellulose* **2008**, *15*, 571–580.
[30] D. Ajò, U. Casellato, E. Fiorin, P. A. Vigato, *J. Cult. Herit.* **2004**, *5*, 333–348.

[31] C. Mazzuca, L. Micheli, R. Lettieri, E. Cervelli, T. Coviello, C. Cencetti, S. Sotgiu, S. Iannuccelli, G. Palleschi, A. Palleschi, *Microchem. J.* **2016**, *126*, 359–367.

[32] R. M. Silverstein, F. X. Webster, D. J. Kiemle, D. L. Bryce, in *Spectrometric Identification of Organic Compounds*, *8th Edition*, John Wiley & Sons, Inc, **2014**, Ch. 3.

[33] Y. Kataoka, T. Kondo, *Macromolecules* **1998**, *31*, 760–764.

[34] F. Jiang, J. L. Dallas, B. K. Ahn, Y.-L. Hsieh, *Carbohydr. Polym.* **2014**, *110*, 360–366.

[35] C. M. Buchanan, K. J. Edgar, J. A. Hyatt, A. K. Wilson, *Macromolecules* **1991**, *24*, 3050–3059.

[36] C. Tang, S. Spinney, Z. Shi, J. Tang, B. Peng, J. Luo, K. C. Tam, *Langmuir* **2018**, *34*, 12897–12905.

[37] E. U. Onche, B. W. Tukura, S. S. Bako, *IOSR J. Appl. Chem.* **2013**, *6*, 45–51.

[38] D. S. Wishart, C. Knox, A. C. Guo, R. Eisner, N. Young, B. Gautam, D. D. Hau, N. Psychogios, E. Dong, S. Bouatra, R. Mandal, I. Sinelnikov, J. Xia, L. Jia, J. A. Cruz, E. Lim, C. A. Sobsey, S. Shrivastava, P. Huang, P. Liu, L. Fang, J. Peng, R. Fradette, D. Cheng, D. Tzur, M. Clements, A. Lewis, A. De Souza, A. Zuniga, M. Dawe, Y. Xiong, D. Clive, R. Greiner, A. Nazyrova, R. Shaykhutdinov, L. Li, H. J. Vogel, I. Forsythe, *Nucleic Acids Res.* **2009**, *37*, D603–D610.

[39] B. Lu, S. Zhen, L. Zhao, G. Zhang, D. Mo, J. Xu, *Synth. Met.* **2014**, *198*, 155–160.

[40] M. d'Ischia, A. Napolitano, V. Ball, C.-T. Chen, M. J. Buehler, *Acc. Chem. Res.* **2014**, *47*, 3541–3550.

[41] Y. Su, Y. Zhao, H. Zhang, X. Feng, L. Shi, J. Fang, *J. Mater. Chem. C* **2017**, *5*, 573–581.

[42] C. Mazzuca, M. Carbone, R. Cancelliere, S. Prati, G. Sciutto, R. Mazzeo, L. Tositti, R. Regazzi, D. Mostacci, L. Micheli, *Microchem. J.* **2018**, *143*, 493–502.

RESEARCH ARTICLE
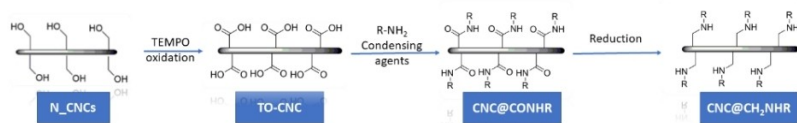
The surface amination of cellulose nanocrystals is a powerful tool to modulate their pH, photoluminescence, or electrochemical activity. This work reports cellulose nanocrystals surface modification and a thorough analysis of their surface structure.

Dr. R. D'Orsi, V. C. Canale, Dr. R. Cancelliere, Dr. O. Hassan Omar, Prof. C. Mazzuca, Prof. L. Micheli, Prof. A. Operamolla*

1 – 10

Tailoring the Chemical Structure of Cellulose Nanocrystals by Amine Functionalization